Collective Dynamics

# Improving Pedestrian Dynamics Predictions Using Neighboring Factors

**Huu-Tu Dang**[1] · **Benoit Gaudou**[1] · **Nicolas Verstaevel**[1]

[1] UMR 5505 IRIT, Université Toulouse Capitole, France
E-mail: {huu-tu.dang, benoit.gaudou, nicolas.verstaevel}@ut-capitole.fr

Received: 16 October 2023 / Last revision received: 24 June 2024 / Accepted: 24 June 2024
DOI: 10.17815/CD.2024.178

**Abstract** Predicting pedestrian dynamics is a complex task as pedestrian speed is influenced by various external factors. This study investigates neighboring factors that can be used to improve pedestrian walking speed prediction accuracy in both low- and high-density scenarios. Different factors are proposed, including Mean Distance, Time-to-Collision, and Front Effect, and data for each factor is extracted from different public datasets. The collected data at time $t$ is used to train a neural network to predict the pedestrian walking speed at time $t + \Delta t$. Predictions are evaluated using the Mean Absolute Error. Our results demonstrate that incorporating the Front Effect significantly improves prediction accuracy in both low- and high-density scenarios, whereas the Mean Distance factor only proves effective in high-density cases. On the other hand, no significant improvement is observed when considering the Time-to-Collision factor. These preliminary findings can be utilized to enhance the accuracy of pedestrian dynamics predictions by incorporating these factors as additional features within the model.

**Keywords** Pedestrian dynamics · speed predictions · neighboring effects · neural network

## 1 Introduction

Predicting pedestrian dynamics is a complex task as pedestrian walking speed is influenced not only by intrinsic factors, such as pedestrian's objectives and characteristics, but also by external factors like social groups [1], crowd density [2], environmental conditions [3, 4], among others. Consequently, incorporating these external factors can improve the accuracy of predicting pedestrian behaviors. For instance, better prediction accuracy in pedestrian trajectories is archived by providing neural networks additional contextual information, such as integrating environmental layouts via hierarchical LSTM-based neural network [5], determining most interactions with neighbors using attention

 

mechanisms [6,7], or including time-to-collision terms into the loss function [8,9]. However, there remains a need to evaluate the impact of these factors, particularly those derived from neighboring pedestrians, on the performance of pedestrian dynamics prediction across different scenarios.

In this article, we propose and investigate different neighboring factors that can be used to improve pedestrian walking speed prediction accuracy in both low- and high-density scenarios. To do this, two types of datasets are prepared corresponding to these scenarios and data is analyzed using a neural network approach.

# 2 Methodology

This section presents data extraction for the proposed neighboring factors from different public datasets and our method to analyze the impact of these factors on predicting pedestrian walking speed.

## 2.1 Data extraction

We propose to investigate the impact of the following external factors derived from neighboring: Mean Distance, Time-to-Collision, and Front Effect. For each pedestrian $i$, the proposed factors are extracted with respect to each neighboring pedestrian $j$ of its **K nearest neighbors**. Let $p_i = (x_i, y_i)$, $v_i = (v_{x_i}, v_{x_j})$, and $r_i$ represent the position, velocity, and radius of the pedestrian $i$, respectively.

The walking speed of pedestrian $i$ is denoted as $\|v_i\|$ where $\|v\|$ represents the Euclidean norm of vector $v$. The relative position and velocity between the pedestrians $i$ and $j$ are denoted as $p_{ij} = (\Delta x_{ij}, \Delta y_{ij}) = (x_i - x_j, y_i - y_j)$ and $v_{ij} = (\Delta v_{x_{ij}}, \Delta v_{y_{ij}}) = (v_{x_i} - v_{x_j}, v_{y_i} - v_{y_j})$, respectively. The description of these factors is as follows:

- **Mean Distance (MD)** is computed as the mean Euclidean distance to each of the K nearest neighbors. The MD represents local density information around the pedestrian; for example, a smaller MD indicates a higher local density level surrounding the pedestrian.

$$d_i^K = \frac{1}{K} \sum_{j=1}^{K} \sqrt{(x_i - x_j)^2 + (y_i - y_j)^2}, \tag{1}$$

- **Time-to-Collision (TTC)** between the two pedestrians $i$ and $j$, denoted as $\tau_{ij}$, is estimated as the remaining time until collision if they continue to move with their current velocities [10]. The TTC is a sufficient indicator to model pedestrian-pedestrian interactions [10] rather than only relative distance. The TTC value is assigned to a large positive number if no collision is anticipated between the two pedestrians. Here, the smallest TTC value in the K nearest neighbors is selected.

$$\tau_{\mathrm{i}}^{\mathrm{K}} = \min_{1 \le j \le K} \tau_{ij} = \min_{1 \le j \le K} \frac{-p_{ij} \cdot v_{ij} - \sqrt{(p_{ij} \cdot v_{ij})^2 - \|v_{ij}\|^2 (\|p_{ij}\|^2 - (r_i + r_j)^2)}}{\|v_{ij}\|^2}, \tag{2}$$

- **Front Effect (FE)** considers the K nearest neighbors who fall in a 180-degree field of vision of the pedestrian $i$. The reason for choosing this factor is that pedestrians are more influenced by neighbors who appear in their immediate field of vision.

$$\mathrm{FE}_{\mathrm{i}}^{\mathrm{K}} = \{\|v_i\|, \Delta x_{ij}, \Delta y_{ij}, \Delta v_{x_{ij}}, \Delta v_{y_{ij}} | 1 \leq j \leq K, 0 \leq \frac{v_i \cdot v_j}{\|v_i\|\|v_j\|} \leq 1\}. \quad (3)$$

In addition to these aforementioned neighboring factors, fundamental information is also extracted, which includes pedestrian speed and its relative position and relative velocity with respect to its neighboring pedestrians.

## 2.2 Datasets

Data is extracted from three widely used public pedestrian datasets using different values of K (3, 5, 7, and 10). The fundamental characteristics of these datasets are presented in Tab. 1. Given that high density is defined as greater than 1 pedestrian/$\mathrm{m}^2$ [11], the datasets are classified as low-density (ETH [12] and UCY [13]) and high-density (FZJ [14]). The framerates of the low-and high-density datasets are 2.5 fps and 16 fps, respectively.

| **Dataset** | **Source** | **Data** | **Setting** | **No. Traj** | **Avg. Density** $(\mathbf{1}/\mathrm{m}^2)$ | **Avg. Min TTC** $(\mathbf{s})$ |
|---|---|---|---|---|---|---|
| Low density | ETH [12] | ETH | Outdoor | 361 | 0.15 | 15.64 |
| | | HOTEL | Outdoor | 389 | 0.13 | 4.82 |
| | UCY [13] | ZARA01 | Outdoor | 148 | 0.21 | 6.30 |
| | | ZARA02 | Outdoor | 204 | 0.27 | 6.71 |
| | | UNIV | Outdoor | 434 | 0.38 | 6.53 |
| High density | JÜLICH [14] | bi_b_03 | Lab | 480 | 1.00 | 4.42 |
| | | bi_b_04 | Lab | 743 | 2.32 | 2.84 |
| | | bi_b_05 | Lab | 643 | 2.64 | 2.57 |
| | | bi_b_06 | Lab | 830 | 3.0 | 2.34 |
| | | bi_b_07 | Lab | 606 | 3.45 | 2.08 |
| | | bi_b_08 | Lab | 703 | 3.78 | 2.27 |

**Table 1** Fundamental characteristics of different datasets.

## 2.3 Method

Our method employs a Multilayer Perceptron (MLP) neural network with $h$ hidden layers to learn data at time $t$ and predict the pedestrian walking speed at time $t + \Delta t$. It has been demonstrated that the MLP neural network is more effective in predicting pedestrian walking speed than classical models based on fundamental diagram [15]. Different inputs are fed into four neural networks:

- The first network is the baseline network whose input consists of the following **fundamental information**: the pedestrian's current speed, relative positions, and relative velocities to the K nearest neighbors.

$$\mathrm{NN}_1^{\mathrm{K}} = \mathrm{MLP}(\|v_i\|, \Delta x_{ij}, \Delta y_{ij}, \Delta v_{x_{ij}}, \Delta v_{y_{ij}} | 1 \leq j \leq K). \tag{4}$$

- In the second neural network, the mean distance of K nearest neighbors is included as an additional feature along with the fundamental information:

$$\mathrm{NN}_2^{\mathrm{K}} = \mathrm{MLP}(\|v_i\|, \Delta x_{ij}, \Delta y_{ij}, \Delta v_{x_{ij}}, \Delta v_{y_{ij}}, d_i^K | 1 \leq j \leq K) \tag{5}$$

- The third neural network incorporates the smallest TTC in the K nearest neighbor as an additional feature along with the fundamental information:

$$\mathrm{NN}_3^{\mathrm{K}} = \mathrm{MLP}(\|v_i\|, \Delta x_{ij}, \Delta y_{ij}, \Delta v_{x_{ij}}, \Delta v_{y_{ij}}, \tau_i^K | 1 \leq j \leq K) \tag{6}$$

- The final neural network uses the fundamental information to the K nearest neighbor in front:

$$\mathrm{NN}_4^{\mathrm{K}} = \mathrm{MLP}(\mathrm{FE}_{\mathrm{i}}^{\mathrm{K}}) \tag{7}$$

The architecture of the MLP neural network is h = (6, 3), meaning there are two hidden layers: the first and second layers contain 6 nodes and 3 nodes, respectively. The input layer size of each neural network depends on the value K in each dataset. Training is conducted separately for low-density and high-density datasets, using the Adam optimizer with a learning rate of 0.001 and the Mean Squared Error as the loss function. Each dataset is split into two subsets, with 80% used for training and 20% used for testing. The Mean Absolute Error (MAE) is used to evaluate the predictions. All computations are performed on an AMD Ryzen 7 4800H CPU with 16 GB of memory.

## 3 Results

For each neural network, the average MAE result is computed from 30 trainings. Then, the average MAE results of the other neural networks are compared with the baseline result of $\mathrm{NN}_1^{\mathrm{K}_0}$ with $\mathrm{K}_0 = 3$ to calculate the improvement percentages:

$$\mathrm{IP}_i^{\mathrm{K}} = -\frac{MAE(\mathrm{NN}_i^{\mathrm{K}}) - MAE(\mathrm{NN}_1^{\mathrm{K}_0})}{MAE(\mathrm{NN}_1^{\mathrm{K}_0})} \times 100\%, \text{ for } i = 1,2,3,4 \text{ and } \mathrm{K} = 3,5,7,10. \tag{8}$$

where $MAE(\mathrm{NN}_i^{\mathrm{K}})$ presents the MAE of actual speed $\|v_j\|$ and the corresponding speed predicted by the neural network $\mathrm{NN}_i^{\mathrm{K}}$ over N data samples:

$$MAE(\mathrm{NN}_i^{\mathrm{K}}) = \frac{1}{N}\Sigma_{j=1}^{N} | \|v_j\| - \hat{v}_j^{\mathrm{NN}_i^{\mathrm{K}}} |. \tag{9}$$

Fig. 1 shows the MAE and improvement percentage results of predictions of different neural networks over different numbers of neighbors in both low-density and high-density datasets. It can be observed from both low-density and high-density datasets that the performance of all neural networks consistently improves when the number of neighbors increases. This trend indicates that including more neighbors provides more contextual information so neural networks can learn better.

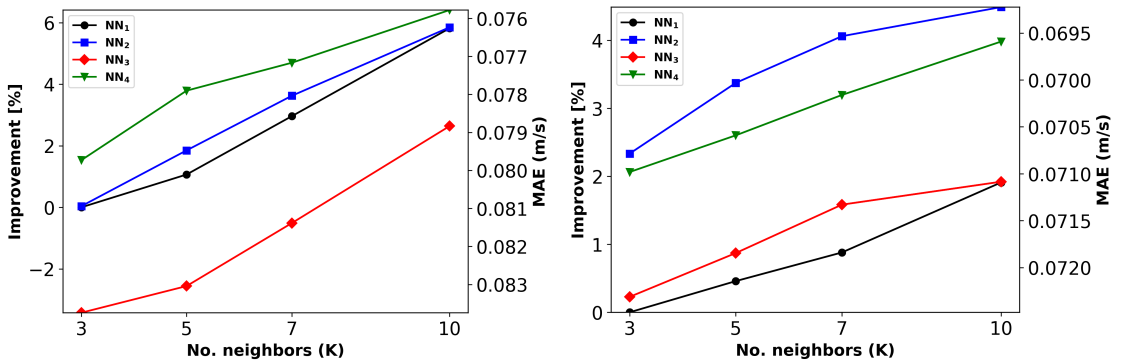


(a) Low-density dataset with $\Delta t = 0.4s$. (b) High-density dataset with $\Delta t = 0.375s$

**Figure 1** Improvement results in (a) Low-density dataset and (b) High-density dataset.

In the low-density dataset (see Fig. 1(a)), adding TTC to the neural networks worsens prediction accuracy. This can be explained by the fact that most of the time-to-collision to neighbors in low-density scenarios is typically large, while the interaction time horizon is 2 – 4s [10]. Consequently, at the macroscopic level, the influence of this factor on pedestrian movement becomes trivial in low-density situations. On the other hand, FE presents the best improvement in prediction accuracy (approximately 5.8% for $\mathrm{NN}_4^{\mathrm{K}}$ with K = 10), while the effect of MD with $\mathrm{NN}_2$ shows similar results with $\mathrm{NN}_1$. This observation suggests that in low-density situations, the FE is the most important factor, while the impact of MD is not particularly meaningful.

In the high-density dataset, adding any proposed neighboring factors to the neural networks helps to improve the results. Using MD and FE shows strong improvements (around 4.5% for $\mathrm{NN}_2^{\mathrm{K}}$ with K = 10 and 4.0 % for $\mathrm{NN}_4^{\mathrm{K}}$ with K = 10), while adding TTC slightly improves prediction accuracy. This suggests that the MD and FE are more effective than TTC in high-density scenarios.

Based on the results above, the two factors that yield the best improvement are Mean Distance and Front Effect and thus are chosen for comparison. For each number of K, the improved accuracy for MD and FE is calculated to the results of the neural network $\mathrm{NN}_1^{\mathrm{K}}$:

$$\mathrm{IP}_{\mathrm{i}}^{\mathrm{K}} = -\frac{MAE(\mathrm{NN}_i^{\mathrm{K}}) - MAE(\mathrm{NN}_1^{\mathrm{K}})}{MAE(\mathrm{NN}_1^{\mathrm{K}})} \times 100\%, \text{ for } i = 2,4 \text{ and } \mathrm{K} = 3,5,7,10. \quad (10)$$

Fig. 2 presents the comparison of improvement percentage between the low- and high-density datasets for Mean Distance and Front Effect over different numbers of K.

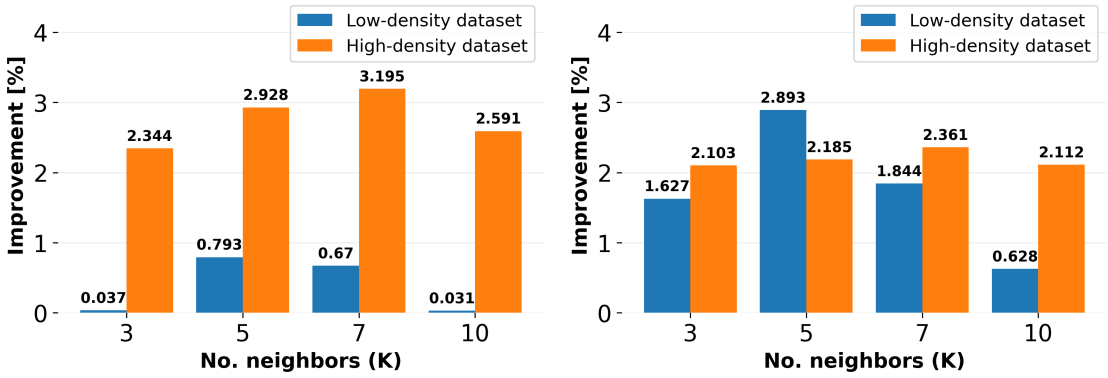


(a) Mean Distance (b) Front Effect

**Figure 2** Comparison of percentage of improved accuracy between low- and high-density datasets over different numbers of K using (a) Mean Distance and (b) Front Effect.

For MD, there is a clear difference in improvement between low- and high-density situations. The improvement in the high-density dataset is much higher than that in the low-density dataset for all different numbers of K neighbors. The lowest and highest improvement in the high-density dataset is 2.344% and 3.195%, respectively, while the highest improvement in the low-density dataset is just 0.793%. This indicates that MD in high-density scenarios provides more information than in low-density scenarios as it describes the local density surrounding pedestrians.

On the other hand, FE exhibits a noticeable improvement in accuracy in both low-density and high-density datasets. The highest improvement in the low-density dataset is 2.893 % with K = 5, while the improvement results remain stable from 2.103 to 2.361% in the high-density dataset. This suggests that pedestrian movement is primarily influenced by the neighboring pedestrians in directional relevance. These preliminary results can be incorporated into the simulation models and neural network algorithms to improve accuracy.

## 4 Conclusion

This paper investigates neighboring factors that can be used to improve pedestrian walking speed prediction accuracy in both low- and high-density scenarios. The data for these factors, collected from various public datasets, is analyzed using a neural network approach. It has been demonstrated that incorporating the appropriate contextual information from the neighboring pedestrians into the neural network's input can significantly improve prediction accuracy. The key finding reveals that the Front Effect is an impactful factor in both scenarios, while Mean Distance becomes particularly crucial only in high-density situations. Another factor is that Time-to-Collision has no significant effect at low density and is trivial at high-density situations. These preliminary findings can be utilized to enhance the accuracy of pedestrian dynamics predictions by incorporating these factors

as additional features within the model.

**Acknowledgements** The authors acknowledge the Franco-German research project MADRAS funded in France by the Agence Nationale de la Recherche (ANR, French National Research Agency), grant number ANR-20-CE92-0033, and in Germany by the Deutsche Forschungsgemeinschaft (DFG, German Research Foundation), grant number 446168800.

**Author Contributions** Huu-Tu Dang: Conceptualization, Methodology, Software, Formal analysis, Data curation, Visualization, Writing - Original draft, Writing - Review and editing / Benoit Gaudou: Conceptualization, Methodology, Writing - Review and editing, Funding acquisition, Supervision / Nicolas Verstaevel: Conceptualization, Methodology, Writing - Review and editing, Funding acquisition, Supervision.

# References

[1] Nicolas, A., Hassan, F.H.: Social groups in pedestrian crowds: review of their influence on the dynamics and their modelling. Transportmetrica A: transport science **19**(1), 1970651 (2023)

[2] Seyfried, A., Steffen, B., Klingsch, W., Boltes, M.: The fundamental diagram of pedestrian movement revisited. Journal of Statistical Mechanics: Theory and Experiment **2005**(10), P10002 (2005)

[3] Franěk, M.: Environmental factors influencing pedestrian walking speed. Perceptual and motor skills **116**(3), 992–1019 (2013)

[4] Meeder, M., Aebi, T., Weidmann, U.: The influence of slope on walking activity and the pedestrian modal share. Transportation research procedia **27**, 141–147 (2017)

[5] Xue, H., Huynh, D.Q., Reynolds, M.: Ss-lstm: A hierarchical lstm model for pedestrian trajectory prediction. In: 2018 IEEE Winter Conference on Applications of Computer Vision (WACV), pp. 1186–1194. IEEE (2018)

[6] Vemula, A., Muelling, K., Oh, J.: Social attention: Modeling attention in human crowds. In: 2018 IEEE international Conference on Robotics and Automation (ICRA), pp. 4601–4607. IEEE (2018)

[7] Peng, Y., Zhang, G., Shi, J., Xu, B., Zheng, L.: Srai-lstm: A social relation attention-based interaction-aware lstm for human trajectory prediction. Neurocomputing **490**, 258–268 (2022)

[8] Dang, H.T., Korbmacher, R., Tordeux, A., Gaudou, B., Verstaevel, N.: Ttc-slstm: Human trajectory prediction using time-to-collision interaction energy. In: 2023 15th International Conference on Knowledge and Systems Engineering (KSE), pp. 1–6. IEEE (2023)

[9] Korbmacher, R., Dang, H.T., Tordeux, A.: Predicting pedestrian trajectories at different densities: A multi-criteria empirical analysis. Physica A: Statistical Mechanics and its Applications **634**, 129440 (2024)

[10] Karamouzas, I., Skinner, B., Guy, S.J.: Universal power law governing pedestrian interactions. Physical review letters **113**(23), 238701 (2014)

[11] Duives, D.C., Daamen, W., Hoogendoorn, S.P.: State-of-the-art crowd motion simulation models. Transportation research part C: emerging technologies **37**, 193–209 (2013)

[12] Pellegrini, S., Ess, A., Schindler, K., Van Gool, L.: You'll never walk alone: Modeling social behavior for multi-target tracking. In: 2009 IEEE 12th international conference on computer vision, pp. 261–268. IEEE (2009)

[13] Lerner, A., Chrysanthou, Y., Lischinski, D.: Crowds by example. In: Computer graphics forum, vol. 26, pp. 655–664. Wiley Online Library (2007)

[14] Cao, S., Seyfried, A., Zhang, J., Holl, S., Song, W.: Fundamental diagrams for multidirectional pedestrian flows. Journal of Statistical Mechanics: Theory and Experiment **2017**(3), 033404 (2017)

[15] Tordeux, A., Chraibi, M., Seyfried, A., Schadschneider, A.: Prediction of pedestrian dynamics in complex architectures with artificial neural networks. Journal of intelligent transportation systems **24**(6), 556–568 (2020)